Available online at www.sciencedirect.com
ScienceDirect
Journal of Catalysis 246 (2007) 362–369
JOURNAL OF CATALYSIS
www.elsevier.com/locate/jcat

A novel method for the synthesis of titania nanotubes using sonoelectrochemical method and its application for photoelectrochemical splitting of water

S.K. Mohapatra, M. Misra *, V.K. Mahajan, K.S. Raja

Materials Science and Metallurgical Engineering, MS 388, University of Nevada, Reno, NV 89557, USA

Received 2 October 2006; revised 18 December 2006; accepted 27 December 2006

Available online 25 January 2007

Abstract

This new method describes the application of sonoelectrochemistry to quickly synthesize well-ordered and robust titanium dioxide (TiO_2) nanotubular arrays. Self-ordered arrays of TiO_2 nanotubes of 30–100 m in diameter and 300–1000 nm in length can be rapidly synthesized under an applied potential of 5–20 V. The rate of formation of the TiO_2 nanotubes by the sonoelectrochemical method is found to be almost twice as fast as the magnetic stirring method. It also demonstrates that high-quality nanotubes can be prepared using high viscous solvents like ethylene glycol under ultrasonic treatment. The TiO_2 nanotubes prepared in the organic electrolytes (ethylene glycol) are then annealed under H_2 atmosphere to give $TiO_{2-x}C_x$ types material having a band gap of around 2.0 eV. This process is found to be highly efficient for incorporating carbon into TiO_2 nanotubes. Various characterization techniques (viz., FESEM, GXRD, XPS, and DRUV–vis) are used to study the morphology, phase, band gap, and doping of the nanotubes. The photoelectrocatalytic activity of these materials to generate H_2 by water splitting is found to be promising at 0.2 V vs Ag/AgCl.

Keywords: TiO_2 nanotubes; Sonoelectrochemistry; Photoelectrocatalysis; Water splitting

1. Introduction

Titania (TiO_2) is well known as a semiconductor with photocatalytic activities and has great potential in many areas, including environmental purification, gas sensors, photovoltaics, immobilization of biomolecules, and generation of hydrogen gas [1–12]. Over the past several years, preparation of TiO_2 nanotubes by the anodization process has caught the attention of the scientific community due to its one-dimensional nature, ease of handling, and simple preparation. Over the years, several electrolytic combinations have been used for the anodization of titanium [13–18]. The anodization of titanium using phosphoric acid and sodium fluoride or hydrofluoric acid has also recently been reported [19]. However, the reported titania nanotubes are not well ordered, and it takes several hours to make micron-length nanotubes in a high-pH electrolyte. This paper presents a novel sonoelectrochemical technique to anodize titania—anodization under irradiation of ultrasonic waves—which quickly leads to the synthesis of well-ordered titania nanotubes. The anodization approach builds self-organized titania nanotubular arrays of controllable tube diameter, good uniformity, and conformability over large areas.

Sonochemistry is widely used for catalysis, electrochemistry, food technology, synthesis of nanomaterials, and water purification, and other applications [20]. Sonochemistry works through generation and subsequent destruction of cavitation bubbles. Collapse of a cavitation bubble on or near to a solid surface generates a powerful liquid jet targeted at the surface. This effect increases mass flow through the nanotubular surface and thus increases the rate of formation of the nanotubes. On the other hand, the formation of the nanotubes using conventional magnetic stirring is retarded by the formation of a double layer and diffusion-limited transport of the species. A better quality

* Corresponding author.
E-mail address: misra@unr.edu (M. Misra).

0021-9517/$ – see front matter
doi:10.1016/j.jcat.2006.12.020

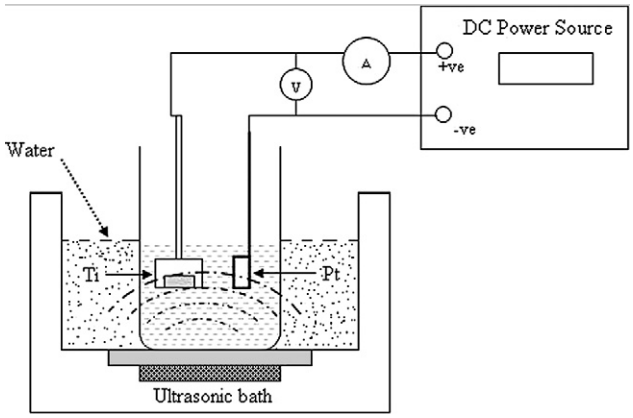

Fig. 1. Experimental setup for anodization of titanium using ultrasonic treatment.

of nanotubes could be obtained through the sonoelectrochemical method, because the mass transfer throughout the process is uniform. The nanotubes synthesized through the sonoelectrochemical route are tested for photoelectrocatalytic generation of H_2 using water splitting and were found to have better activity than the materials prepared by the magnetic stirring technique.

2. Experimental

2.1. Chemicals

Phosphoric acid (H_3PO_4, Sigma–Aldrich, 85% in water), sodium fluoride (NaF, Fischer, 99.5%), potassium fluoride (KF, Aldrich, 98%), ammonium fluoride (NH_4F, Fischer, 100%), ethylene glycol (EG, Fischer), and potassium hydroxide (KOH) were used.

2.2. Preparation of TiO_2 nanotubular arrays

Anodization of titanium was carried out by modifying an earlier reported procedure [19]. 16 mm discs are punched out from a stock of Ti foil (0.2 mm thick, 99.9% purity, ESPI-metals, USA), washed in acetone, and secured in a polytetrafluoroethylene (PTFE) holder exposing only a 0.7 cm^2 area to the electrolyte. Nanotubular TiO_2 arrays were formed by anodization of the Ti foils in 300 ml of electrolytic solution using ultrasonic waves (100 W, 42 kHZ, Branson 2510R-MT). Various electrolytic combinations were used for this purpose in both aqueous and nonaqueous media.

A two-electrode configuration was used for anodization (Fig. 1). A flag shaped platinum (Pt) electrode (thickness: 1 mm, area: 3.75 cm^2) served as a cathode. The distance between the two electrodes was kept at 4.5 cm in all experiments. Anodization was carried out by varying the applied potential from 5 to 20 V using a rectifier (Agilent, E3640A). During anodization, instead of a magnetic stirrer, ultrasonic waves were irradiated onto the solution to enhance the mobility of the ions inside the solution. The anodization current was monitored continuously using a digital multimeter (METEX, MXD 4660A). After an initial increase-decrease transient, the current reached a steady-state value. The anodized samples were properly washed with distilled water to remove the occluded ions from the anodized solutions, dried in an air oven, and processed for characterization. The ultrasonic-mediated, magnetically stirred, anodized titanium samples are designated in the main text as UAT and SAT, respectively.

2.3. Annealing of the materials

The anodized titania nanotubular arrays were annealed in a nitrogen and oxygen atmosphere at 500 °C for 6 h in a CVD furnace at a heating rate of 1 °C/min. The UAT samples annealed under these conditions are designated N_2-UAT and O_2-UAT. The TiO_2 nanotubes prepared by magnetic stirring and annealed under N_2 are designated N_2-SAT. The TiO_2 nanotubes prepared using ethylene glycol were annealed using 20% hydrogen under an argon atmosphere at 625 °C for 60 min.

2.4. Characterization

A field emission scanning electron microscope (FESEM; Hitachi, S-4700) was used to analyze the nanotube formation and morphology. Energy-dispersive spectroscopy (EDS) (at 20 V) was used for elemental analysis. Diffuse reflectance ultraviolet and visible (DRUV–vis) spectra of TiO_2 samples were measured from the optical absorption spectra using a UV–vis spectrophotometer (UV-2401 PC, Shimadzu). Fine $BaSO_4$ powder was used as a standard for baseline and the spectra are recorded in a range 200–800 nm. Further characterization of the TiO_2 nanotubes was carried out by high-resolution X-ray photoelectron spectroscopy (XPS, Surface Science Instruments) using a focused monochromatic Al$K\alpha$ X-ray source and a hemispherical sector analyzer operated in fixed analyzer transmission mode. Surveys were run with a pass energy of 25 eV and the take-off angle is 35°. Glancing angle X-ray diffraction (GXRD) was done using a Philips-12045 B/3 diffractometer. The target used in the diffractometer was copper ($\lambda = 1.54$ Å), and the scan rate was 1.2 deg/min.

2.5. Photoelectrochemical generation of hydrogen from water

Experiments on H_2 generation by photoelectrolysis of water were carried out in a glass cell with photoanode (nanotubular TiO_2 specimen) and cathode (Platinum foil) compartments. The compartments were connected by a fine porous glass frit. The reference electrode (Ag/AgCl) was placed closer to the anode using a salt bridge (saturated KCl)-Luggin probe capillary. The cell was provided with a 60-mm diameter quartz window for light incidence. The electrolyte used was 1 M KOH. A computer-controlled potentiostat (SI 1286, England) was used to control the potential and record the photocurrent generated. A 300-W solar simulator (69911, Newport-Oriel Instruments, USA) was used as a light source. The samples were anodically polarized at a scan rate of 5 mV/s under illumination, and the photocurrent was recorded.

3. Results and discussion

3.1. Anodization using aqueous acidic solution

The first set of experiments was done to monitor the growth of nanotubes with increasing anodization time. The anodizing solution used for the experiments consisted of 0.5 M H_3PO_4 and 0.14 M NaF. The experiments were carried out at room temperature (22–25 °C), with an anodization voltage of 20 V. The growth of the TiO_2 nanotubes was monitored by taking FESEM (Fig. 2) images at various time intervals.

Fig. 2 shows that after 120 s of anodization, small pits started to form on the surface of titanium. These pits increased in size after 600 s, although still retaining the interpore areas. A 300-nm-thick nanotubular layer film was obtained after 900 s, and after 1200 s the surface was completely filled with well-ordered nanotubes. The average diameter of these nanotubes was around 100 nm, tube length was 600–650 nm, and tube wall thickness was 15–20 nm. The barrier layer (junction between the nanotubes and the metal surface) appeared in the form of domes connected with one another (Fig. 2). No further changes in nanotubular morphology were seen when the anodization was carried out for up to 3 h, due to the formation of a barrier layer after 1200 s.

Carrying out the above experiments under magnetic stirring produced a disordered pore surface after 1500 s, with ordered nanotubes finally formed only after 2700 s [19]. The length of the nanotubes was around 400–500 nm.

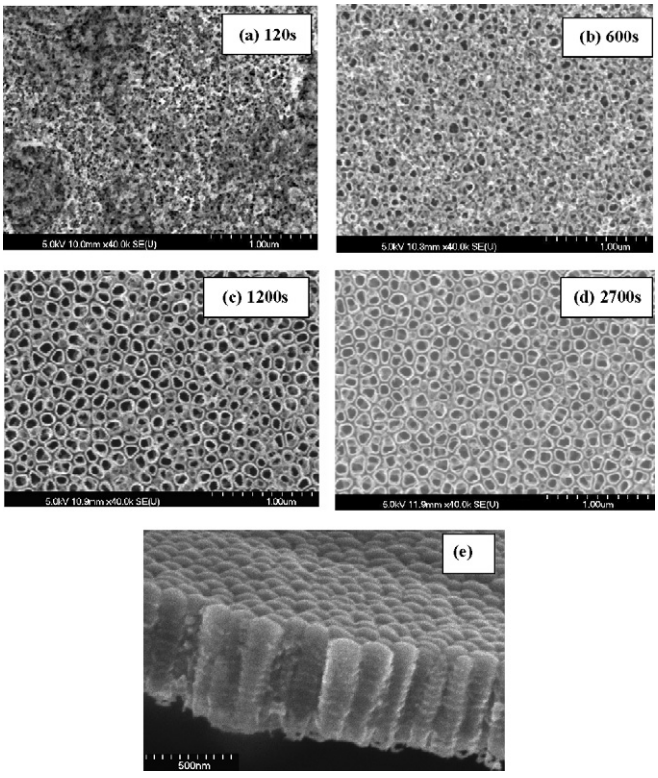

Fig. 2. FESEM images showing different stages of nanotubular TiO_2 film formation during anodization at 20 V in 0.5 M H_3PO_4 + 0.14 M NaF solution with ultrasonic waves irradiation (a–d) and (e) cross-sectional view of (c) showing the compact nanotubes and the barrier layer.

The above experiments show that using ultrasonic waves for anodization can reduce the synthesis time by up to 50% and increase the length of the nanotubes to 600–650 nm. Fig. 2 shows that that TiO_2 nanotubes prepared by the ultrasonic method have a narrow pore size distribution (maximum number of nanotubes in the same pore diameter range), are more compact (nanotubes are well attached to each other), and are one-dimensionally oriented (straight) than the nanotubes prepared by magnetic stirring [19].

The formation mechanism of the TiO_2 nanotubes can be explained as follows [17]. In aqueous acidic medium, titanium oxidizes to form TiO_2,

$$\mathrm{Ti} + 2\mathrm{H_2O} \rightarrow \mathrm{TiO_2} + 4\mathrm{H^+}. \quad (1)$$

The pit initiation on the oxide surface is a complex process. Although TiO_2 is stable thermodynamically at a pH range 2–12, a complexing ligand (F^-) leads to substantial dissolution. The pH of the electrolyte is a deciding factor. The mechanism of pit formation due to F^- ions is given by

$$\mathrm{TiO_2} + 6\mathrm{F^-} + 4\mathrm{H^+} \rightarrow [\mathrm{TiF_6}]^{2-} + 2\mathrm{H_2O}. \quad (2)$$

This complex formation leads to breakage in the passive oxide layer, with pit formation continuing until repassivation occurs [17,19]. Nanotube formation goes through the diffusion of F^- ions and simultaneous effusion of the $[TiF_6]^{2-}$ ions. The faster rate of formation of TiO_2 nanotubes using ultrasonic waves can be explained by the faster mobility of the F^- ions into the nanotubular reaction channel and effusion of the $[TiF_6]^{2-}$ ions from the channel.

It is well known that the cavitation effect of ultrasonication results in implosion of bubbles near the solid surface [20]. Collapse of transient bubbles causes a jet of liquid to impinge on the surface [20]. At a microscopic scale, impingement of a liquid jet on the surface could increase the dissolution reaction rate. Ultrasonication helps break the double layer and thus hastens the diffusion of F^- ions into the nanotubes and effusion of $[TiF_6]^{2-}$ ions from the nanotubes. The higher rate is further confirmed from current versus time plots in Fig. 3. It can be

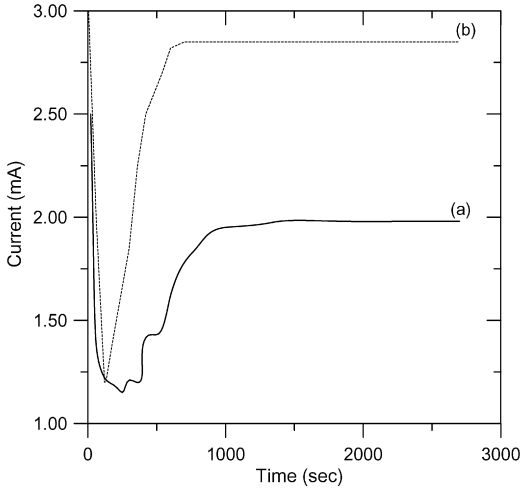

Fig. 3. Current vs time graph during anodization of Ti in 0.5 M H_3PO_4 and 0.14 M NaF solution using (a) magnetic stirring and (b) ultrasonic.

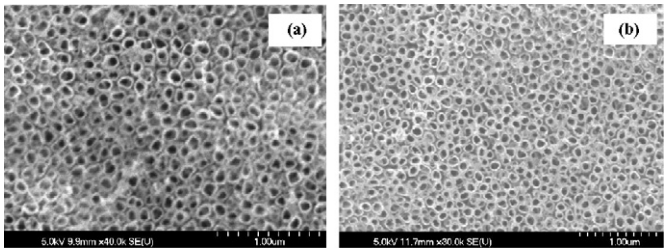

Fig. 4. FESEM images of nanotubular TiO_2 prepared by sonoelectrochemical method using 0.5 M H_3PO_4 and 0.14 M fluoride salt solution: (a) NH_4F and (b) KF.

seen that the current observed in the case of anodization using ultrasonication is almost double that of anodization using magnetic stirring. Also note that the current saturates within 500–600 s when using ultrasonication, compared with 1000–1200 s when using magnetic stirring. The saturation of current with time indicates the development of repassivation, the saturation of nanotube formation. These results are in line with the findings of our FESEM studies (Fig. 2). Anodization of titanium using other fluoride sources, such as ammonium fluoride and potassium fluoride, were also carried out using ultrasonic waves. The FESEM images in Fig. 4 show that the TiO_2 nanotube length and pore diameter for NH_4F and KF are almost similar to those for NaF under the same anodization conditions.

In the next set of experiments, the applied potential was varied from 5 to 20 V by keeping the electrolytic solution (0.5 M H_3PO_4 + 0.14 M NaF) and time (1200 s) constant. All of the experiments were performed under ultrasonic waves. As Fig. 5 shows, TiO_2 nanotubes can be prepared by applying 10–15 V under these experimental conditions. Anodization of Ti at 5 V for 1200 s did not give TiO_2 nanotubes; however, anodization for 2800 s did form TiO_2 nanotubes (Fig. 5). The pore diameter of the titania nanotubes decreased with a decrease in

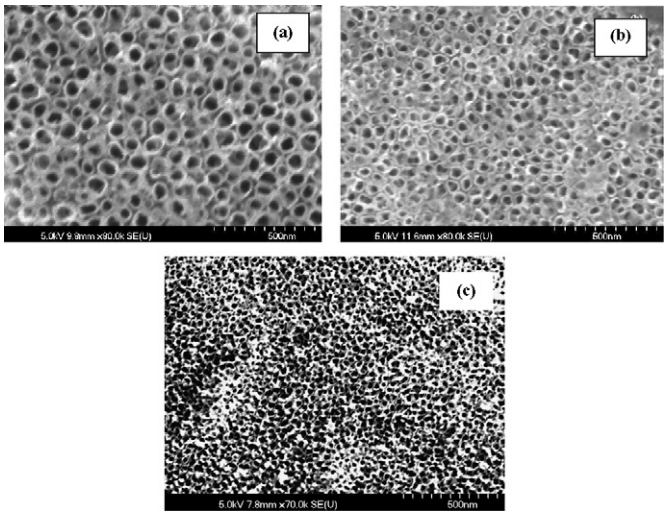

Fig. 5. FESEM images of TiO_2 tubes prepared by sonoelectrochemical method using 0.5 M H_3PO_4 and 0.14 M NaF solution at: (a) 15, (b) 10, and (c) 5 V.

applied potential (Fig. 6). The above observations demonstrate that the pore openings of the TiO_2 nanotubes can be tuned as required by changing the synthesis parameters. A similar observation was reported by Bauer et al. in a detailed study on anodization of titanium with phosphoric acid and hydrofluoric acid [21].

3.2. Anodization using ethylene glycol medium

The next set of experiments was carried out using ethylene glycol and 0.5 wt% of ammonium fluoride solution. Fig. 7 shows that the sonoelectrochemical synthesis of titania nanotubes using ethylene glycol as solvent yielded very-high-quality ordered (hexagonal) nanotubes with very small (40–

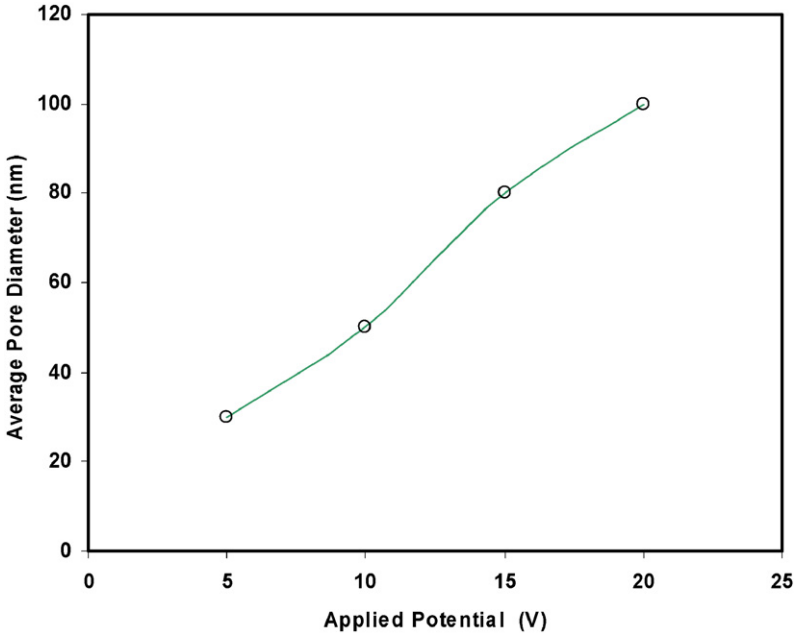

Fig. 6. Effect of applied potential on the pore diameter of the TiO_2 nanotubular structure prepared by sonoelectrochemical method using 0.5 M H_3PO_4 and 0.14 M NaF solution.

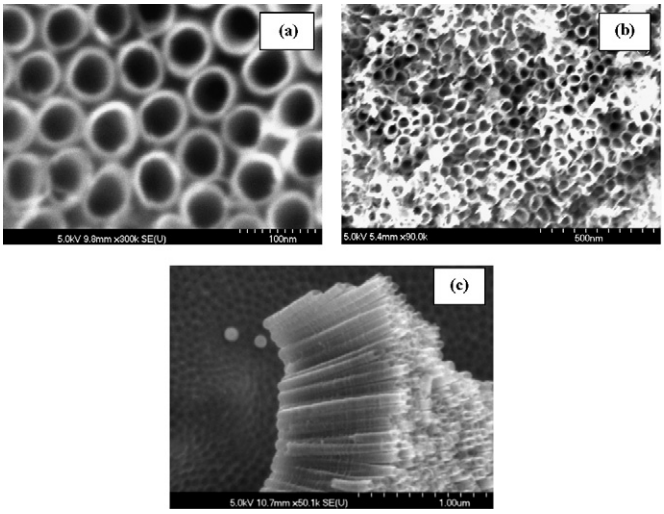

Fig. 7. FESEM images of TiO_2 nanotubular arrays prepared by sonoelectrochemical method using ethylene glycol and 0.5 wt% NH_4F solution: (a) ultrasonic, (b) magnetic stirring, and (c) cross-sectional view of (a).

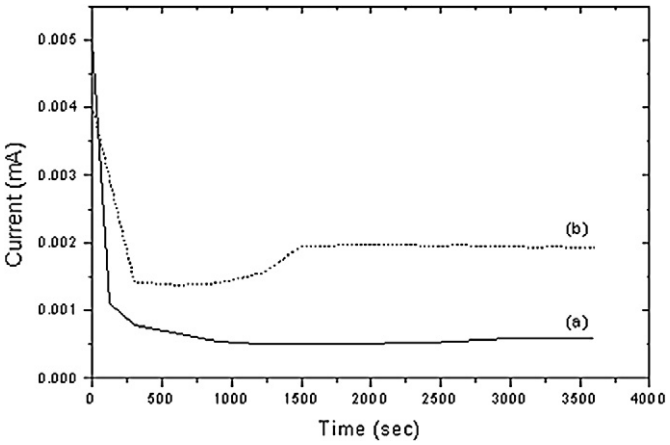

Fig. 8. Current vs time graph during anodization of Ti in ethylene glycol and 0.5 wt% NH_4F solution: (a) magnetic stirring and (b) ultrasonic.

50 nm) pore openings. The nanotubular length was 1 μm when the anodization was carried out at 20 V for 3600 s. For comparison, one experiment was also carried out using ethylene glycol under the magnetic stirring conditions. Fig. 8 compares the current profile of the ultrasonic and magnetic stirring (same area is exposed to the electrolytic surface) and reveals a higher current density for the sonoelectrochemical method compared with anodization using magnetic stirring. This indicates that the sonoelectrochemical method provides more rapid titania nanotube formation. This is further confirmed by the FESEM images of the nanotubes, with 600-nm tubes obtained after 3600 s of anodization.

3.3. Characterization

The as-prepared TiO_2 nanotubular materials were found to be amorphous in nature (GXRD); similar results have been reported by Grimes et al. [22] and Schmuki et al. [23]. The materials were annealed in various temperatures and gaseous atmospheres to transfer the amorphous TiO_2 nanotubes to crystalline materials. A representative XRD pattern of TiO_2 nanotubes annealed under N_2 atmosphere at 500 °C given in Fig. 9 shows predominantly anatase TiO_2 [9,22,23].

DRUV–vis spectra of the as-anodized and annealed titania nanotubes are shown in Fig. 10. It can be seen that the titania nanotubes annealed under N_2 atmosphere give better absorption in a visible region (band gap, 2.8–2.9 eV) compared with the samples annealed under O_2 (band gap, 3.1–3.2 eV). This may

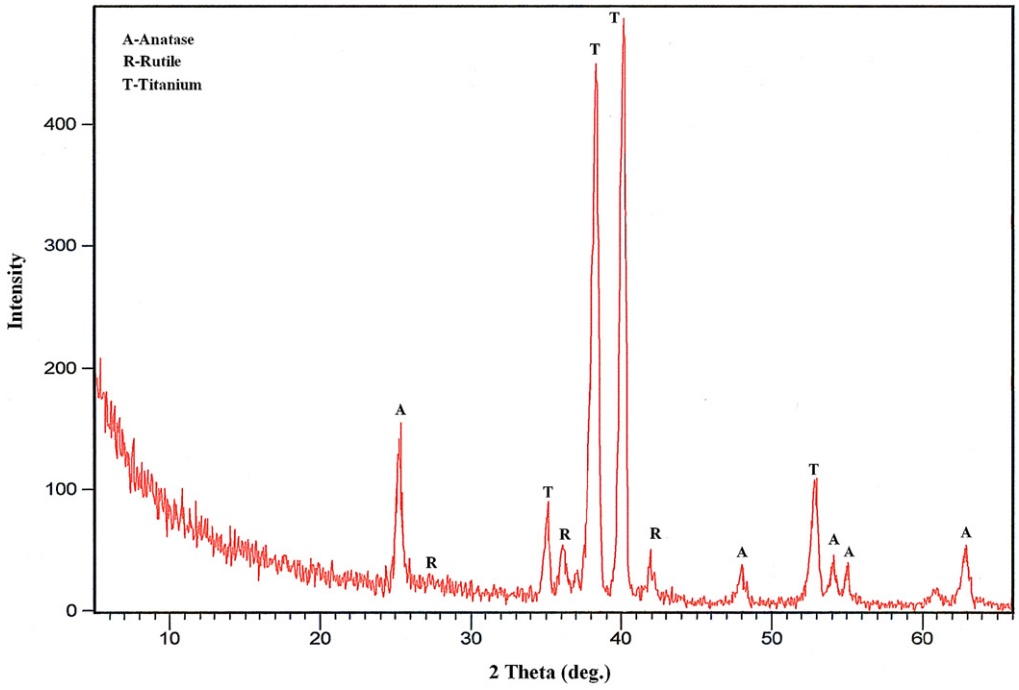

Fig. 9. GXRD pattern of TiO_2 nanotubular arrays prepared by sonoelectrochemical method using 0.5 M H_3PO_4 and 0.14 M NaF solution at 20 V for 1200 s and annealed under H_2 at 500 °C.

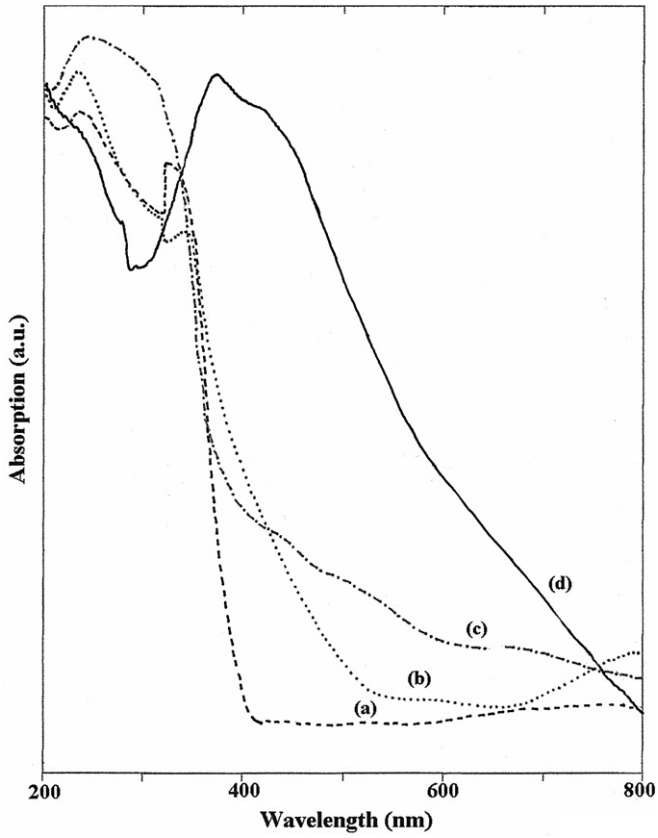

Fig. 10. DRUV–vis spectra of (a) O_2 annealed UAT, (b) N_2 annealed UAT, (c) as-prepared UAT, and (d) H_2 annealed TiO_2 nanotubes prepared using ethylene glycol and ultrasonic treatment.

be due to partial incorporation of nitrogen into the TiO_2 matrix and formation of Ti–N type species, which are responsible for a red shift in the absorption band [24].

A DRUV–vis spectra of samples prepared using ethylene glycol and annealed under H_2 gave maximum absorption in the visible region (Fig. 10). A large red-shift also occurred for the Ti–O charge transfer transition after incorporation of carbon into the TiO_2 nanotubes (band gap, 1.9–2.1 eV). This phenomenon, well documented in the literature, is known as band gap engineering [25,26]. To verify the incorporation of carbon into the TiO_2 nanotubes, it was further characterized using XPS. Fig. 11 shows a typical C1s XPS spectrum of a TiO_2 nanotubular sample prepared by the sonoelectrochemical method using ethylene glycol and annealed under H_2. The spectrum shows a broad asymmetric peak in the range 283–290 eV. The peak can be deconvoluted into two peaks at around 285 and 287.1 eV, corresponding to graphitized carbon and doped carbonate type species, respectively [27–29]. This confirms the incorporation of carbon into the titania nanotubes and production of $TiO_{2-x}C_x$ types of material. It is also noteworthy that the extent of carbon doping by this method (62%) exceeds that in an earlier report on carbon incorporation through acetylene cracking (13%) [9].

3.4. Photoelectrochemical generation of hydrogen by water splitting

Fig. 12 summarizes the results of electrochemical hydrogen generated in terms of the photocurrent of the as-anodized and annealed TiO_2 samples using simulated 1 sunlight intensity.

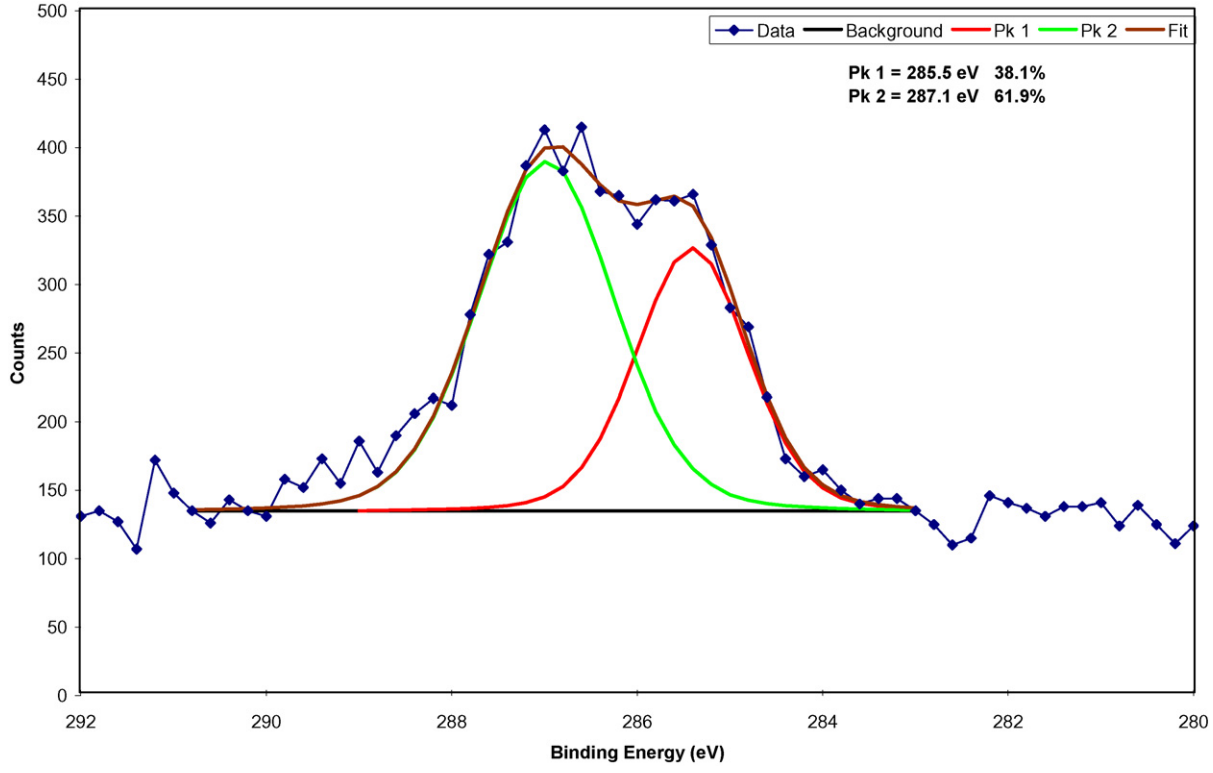

Fig. 11. C1s XPS analysis of carbon doped TiO_2 nanotubes prepared by sonoelectrochemical method using ethylene glycol and 0.5 wt% of NH_4F and annealed under H_2.

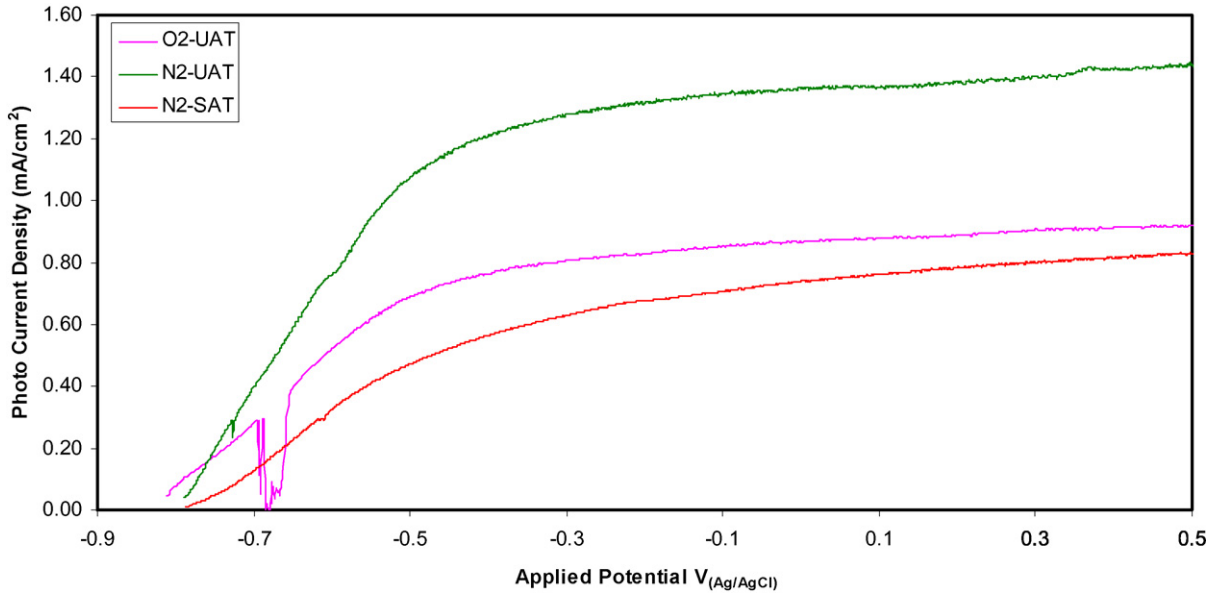

Fig. 12. Photocurrent observed by various catalysts prepared by sonoelectrochemical method and magnetic stirring of various treated TiO_2 nanotubular arrays for water splitting.

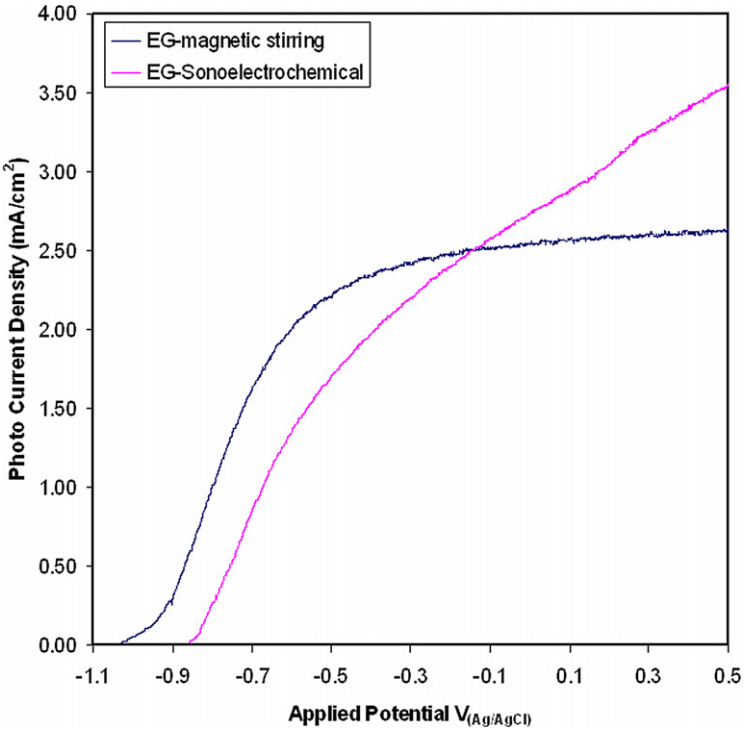

Fig. 13. Photo current generated by TiO_2 nanotubes prepared using ethylene glycol and 0.5 wt% NH_4F solution.

Under anodically polarized conditions, the dark current density (without illumination) was always <0.001 mA/cm^2 for all samples. In as-anodized conditions, the nanotubes of TiO_2 are considered amorphous, and hence the photoelectroactivity was very low (~0.15 mA/cm^2) at 0.2 V vs the Ag/AgCl electrode. Similar results were also reported by Mor et al. for amorphous titania nanotubes [30]. However, the annealed titania nanotubes are crystalline (mostly anatase) and show varied activity depending on the material preparation and annealing atmosphere (Fig. 12).

Titania nanotubes prepared by the sonoelectrochemical method and annealed under N_2 atmosphere (N_2-UAT) gave better photocurrent (1.35 mA/cm^2 at 0.2 V vs Ag/AgCl) compared with those annealed under O_2 atmosphere (O_2-UAT, 0.6 mA/cm^2). This may be due to the lower band gap of the former. On the other hand, TiO_2 nanotubes prepared using ethylene glycol and annealed under H_2 gave excellent activity (3.3 mA/cm^2; Fig. 13). This is due to the lower band gap of carbon-doped titania nanotubes compared with N_2- and O_2-annealed nanotubes. The lower the band gap of the titania

nanotubes, the better the activity for water-splitting. Comparing the activity of the titania nanotubes prepared using the sonoelectrochemical method with that of nanotubes prepared using magnetic stirring (Figs. 12 and 13) show better activity in the former. This better activity is due either to the higher percentage of anatase (GXRD; Fig. 9) in the material, which aids absorption of the illuminated light, or to better heteroatom doping (DRUV–vis and XPS; Figs. 10 and 11) into the TiO_2 nanotubes.

4. Conclusion

From the foregoing discussion, it can be concluded that the sonoelectrochemical method is a highly efficient technique for quickly synthesizing highly ordered titania nanotubes. The pore diameter and nanotube length also can be tuned by changing the applied potential and anodization time. The present study also has demonstrated that the sonoelectrochemical method using ethylene glycol as a solvent can be used to synthesize highly ordered TiO_2 nanotube arrays and incorporate carbon into titania nanotubes. Carbon incorporation by this method was found to be more efficient than carbon incorporation from gases, such as acetylene. Furthermore, these TiO_2 nanotubular catalysts were found to be highly efficient for water-splitting using photoelectrochemical methods under the illumination of sunlight. N_2-annealed TiO_2 nanotubes were found to be more efficient for water-splitting compared with nanotubes annealed under O_2. However, carbon-incorporated titania nanotubes prepared by the sonoelectrochemical method using ethylene glycol were found to be highly promising for water-splitting compared with others. These methods for the synthesis of highly ordered nanotubes can be extended to other metal systems as well.

Acknowledgments

This work was sponsored by the U.S. Department of Energy through grant DE-FC36-06GO86066. The authors thank Gautam Priyadharshan and Dr. Mo Ahmadian for their help with in the experimental work.

References

[1] S. Liu, A. Chen, Langmuir 21 (2005) 8409–8413.
[2] D.V. Bavykin, E.V. Milsom, F. Marken, D.H. Kim, D.H. Marsh, D.J. Riley, F.C. Walsh, K.H. El-Abiary, A.A. Lapkin, Electrochem. Commun. 7 (2005) 1050–1058.
[3] D.V. Bavykin, A.A. Lapkin, P.K. Plucinski, J.M. Friedrich, F.C. Walsh, J. Catal. 235 (2005) 10–17.
[4] G.K. Mor, K. Shankar, M. Paulose, O.K. Varghese, C.A. Grimes, Nano Lett. 5 (2005) 191–195.
[5] J.H. Park, S. Kim, A.J. Bard, Nano Lett. 6 (2006) 24–28.
[6] K.S. Raja, V.K. Mahajan, M. Misra, J. Power Sources 159 (2006) 1258–1265.
[7] P. Pillai, K.S. Raja, M. Misra, J. Power Sources 161 (2006) 524–530.
[8] T. Gandhi, K.S. Raja, M. Misra, Electrochim. Acta 51 (2006) 5932–5942.
[9] K.S. Raja, M. Misra, V.K. Mahajan, T. Gandhi, P. Pillai, S.K. Mohapatra, J. Power Sources 161 (2006) 1450–1457.
[10] J.M. Macak, H. Tsuchiya, A. Ghicov, P. Schmuki, Electrochem. Commun. 7 (2005) 1133–1137.
[11] A. Fujishima, K. Honda, Nature 238 (1972) 37–38.
[12] A.J. Bard, Science 207 (1980) 139–144.
[13] J. Zhao, X. Wang, R. Chen, L. Li, Solid State Commun. 134 (2005) 705–710.
[14] C. Ruan, M. Paulose, O.K. Varghese, G.K. Mor, C.A. Grimes, J. Phys. Chem. B 109 (2005) 15,754–15,759.
[15] J.M. Macak, K. Sirotna, P. Schmuki, Electrochim. Acta 50 (2005) 3679–3684.
[16] H. Tsuchiya, J.M. Macak, L. Taveira, E. Balaur, A. Ghicov, K. Sirotna, P. Schmuki, Electrochem. Commun. 7 (2005) 576–580.
[17] J.M. Macak, H. Tsuchiya, P. Schmuki, Angew. Chem. Int. Ed. 44 (2005) 2100–2102.
[18] Q. Cai, M. Paulose, O.K. Varghese, C.A. Grimes, J. Mater. Res. 20 (2005) 230–236.
[19] K.S. Raja, M. Misra, K. Paramguru, Electrochim. Acta 51 (2005) 154–165.
[20] T.J. Mason, J.P. Lorimer, Sonochemistry: Theory, Applications and Uses of Ultrasound in Chemistry, Ellis Horwood, Chichester, 1988, p. 74.
[21] S. Bauer, S. Kleber, P. Schmuki, Electrochem. Commun. 8 (2006) 1321–1325.
[22] O.K. Varghese, D. Gong, M. Paulose, C.A. Grimes, E.C. Dickey, J. Mater. Res. 18 (2003) 156–165.
[23] R. Beranek, H. Tsuchiya, T. Sugishima, J.M. Macak, L. Taveira, S. Fujimoto, H. Kisch, P. Schmuki, Appl. Phys. Lett. 87 (2005) 243114.1–243114.3.
[24] R. Asahi, T. Morikawa, T. Ohwaki, K. Aoki, Y. Taga, Science 293 (2001) 269–271.
[25] S.U.M. Khan, M. Al-Shahry, W.B. Ingel Jr., Science 297 (2002) 2243–2245.
[26] E. Barborini, A.M. Conti, I. Kholmanov, P. Piseri, A. Podesta, P. Milani, C. Cepek, O. Sakho, R. Macovez, M. Sancrotti, Adv. Mater. 17 (2005) 1842–1846.
[27] C.D. Wagner, W.M. Riggs, L.E. Davis, J.F. Moulder, in: G.E. Muilenberg (Ed.), Handbook of X-ray Photoelectron Spectroscopy, Perkin–Elmer, Norwalk, CT, 1979.
[28] S. Sakthivel, H. Kisch, Angew. Chem. Int. Ed. 42 (2003) 4908–4911.
[29] Y. Li, D.-S. Hwang, N.H. Lee, S.-J. Kim, Chem. Phys. Lett. 404 (2005) 25–29.
[30] M. Paulose, G.K. Mor, O.K. Varghese, K. Shankar, C.A. Grimes, J. Photochem. Photobiol. A Chem. 178 (2006) 8–15.